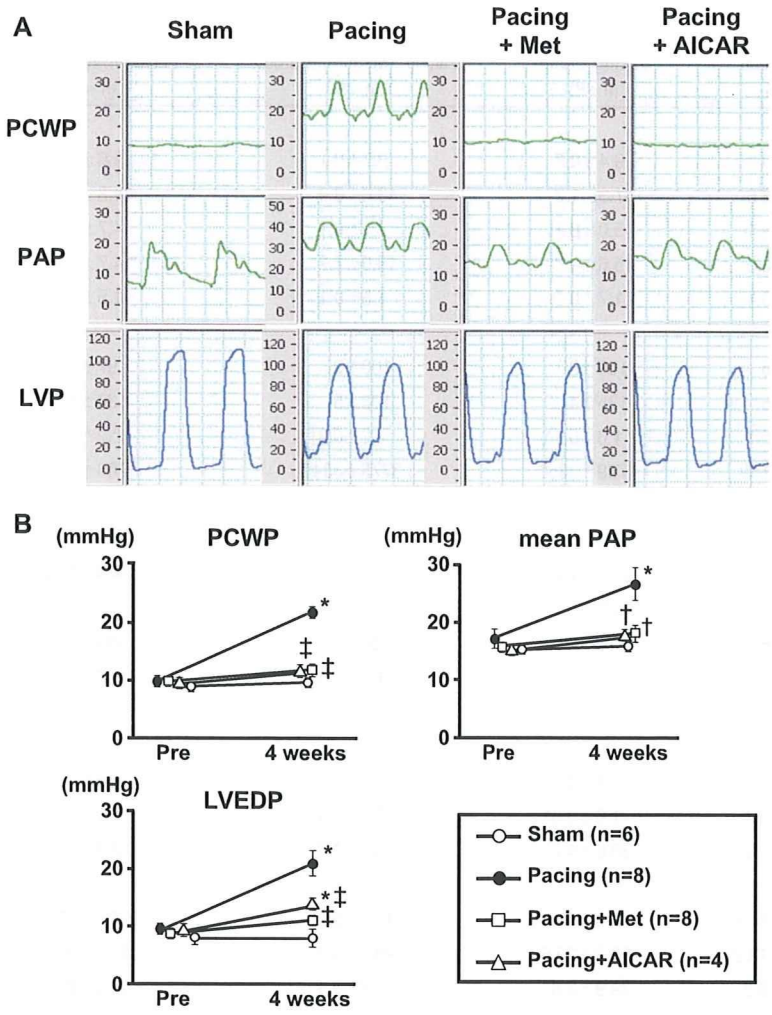

Figure 4. Effect of metformin on hemodynamic parameters. A, Representative graphs of hemodynamic parameters obtained at 4 weeks. B, Hemodynamic parameters before and after the 4-week study period in the sham (n=6), pacing (n=8), pacing plus metformin (n=8), and pacing plus AICAR (n=4) groups. Values are mean±SEM. PAP indicates pulmonary artery pressure; PCWP, pulmonary capillary wedge pressure; and LVEDP, LV end-diastolic pressure. *$P<0.05$ vs sham group; †$P<0.05$ vs pacing group; ‡$P<0.01$ vs pacing group.

Furthermore, we provide sufficient insight because dogs can be monitored more precisely for hemodynamic data than rodents.

Possible Cardioprotective Mechanism of Metformin Mediated via AMPK

Metformin has previously been shown to reduce high fat–induced apoptosis,[23] and AMPK has been reported to protect against hypoxic apoptosis in cardiomyocytes through attenuation of endoplasmic reticulum stress.[24] Consistent with these previous reports, we confirmed that metformin could ameliorate oxidative stress–induced apoptosis in cardiomyocytes. This effect was blunted by compound C, an AMPK inhibitor, suggesting that activation of AMPK was responsible for the inhibition of cardiomyocyte apoptosis. Furthermore, using a dog model, we demonstrated that metformin ameliorated the progression of heart failure induced by rapid RV pacing and decreased apoptosis in the LV myocardium, as indicated by TUNEL staining. Interestingly, AICAR, another AMPK activator, had effects almost identical to those of metformin, supporting that the activation of AMPK contributed to the observed cardioprotective effect. Indeed, AICAR also has been reported to reduce myocardial ischemia/reperfusion injury in humans and animals.[25,26] What processes following AMPK activation are involved in cardioprotection?

The first possibility is enhancement of NO production. Recchia et al[27] reported that basal cardiac NO release is decreased in dogs with heart failure induced by rapid pacing. We found that the difference in plasma NO levels between baseline and 4 weeks of RV pacing was significantly increased by metformin treatment compared with the pacing group. Metformin has been shown to phosphorylate AMPK at Thr-172 in cardiomyocytes and murine hearts,[4,5] whereas AMPK is known to phosphorylate eNOS at Ser-1177 in rat hearts,[28] resulting in an increase in NO production. Indeed, a recent report has indicated that short-term metformin treatment protects against myocardial infarction via AMPK-eNOS–mediated signaling in mice.[7] Other studies have suggested involvement of the AMPK-eNOS pathway in the response of endothelial cells to shear stress,[29] metformin,[30] and statins.[31] Consistent with these reports, we found that either metformin or AICAR promoted the phosphorylation of eNOS at Ser-1177 and increased both mRNA and protein levels of eNOS, possibly leading to increased plasma NO levels and reduced systemic vascular resistance. Although the precise mechanism of the effects of phosphorylation of AMPK by either metformin or AICAR on eNOS protein expression is not clear, these findings suggest that metformin or AICAR increased NO production, which improves endothelial

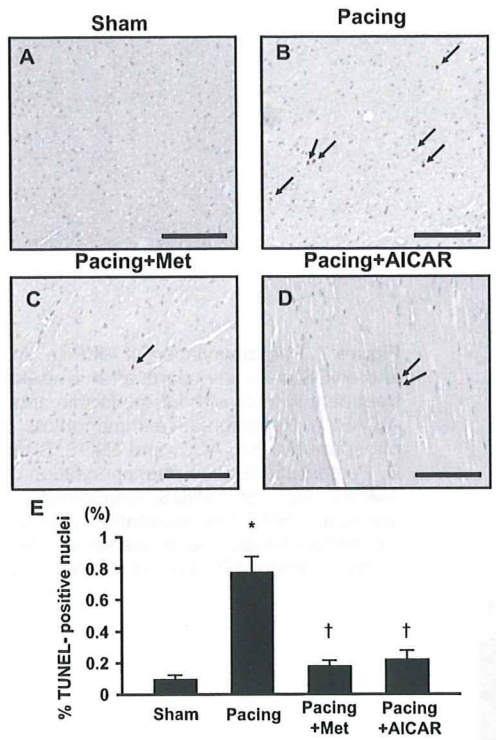

Figure 5. TUNEL staining of canine hearts at 4 weeks. Representative examples of TUNEL-stained hearts from sham (A), pacing (B), pacing plus metformin (C), and pacing plus AICAR (D) groups. Arrows indicate TUNEL-positive nuclei (brown). Scale bar=100 μm. E, Quantitative data on the percentage of TUNEL-positive nuclei to total cell nuclei. *$P<0.05$ vs sham group; †$P<0.05$ vs pacing group.

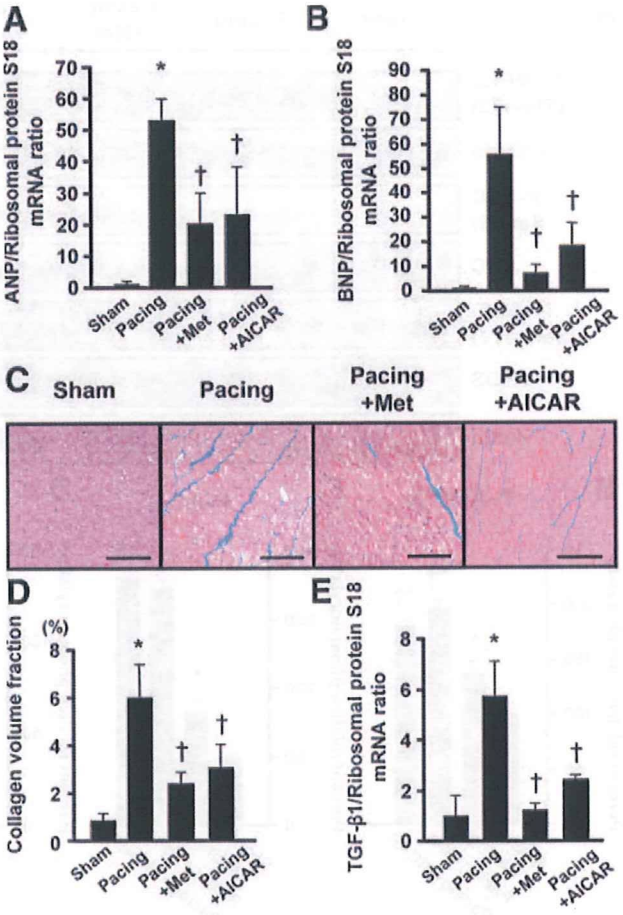

Figure 6. Natriuretic peptide expression, cardiac collagen volume fraction, and TGF-β1 expression. A, B, and E, Quantitative real-time reverse-transcriptase polymerase chain reaction analysis of myocardial atrial natriuretic peptide (ANP), brain natriuretic peptide (BNP), and TGF-β1 expression, respectively. The mRNA values were corrected for the ribosomal protein S18 mRNA level. The sham group was arbitrarily assigned a value of 1.0. Results are mean±SEM. Representative results from 3 independent experiments are shown. *$P<0.05$ vs sham group; #$P<0.05$ vs pacing group. C, Representative histological appearance of LV myocardium stained with Masson's trichrome stain (light blue). Scale bar=100 μm. D, Collagen volume fraction in the LV myocardium. Values are mean±SEM. *$P<0.05$ vs sham group; †$P<0.05$ vs pacing group.

function. NO is believed to have various cardioprotective effects.[16] Therefore, enhancement of NO production by metformin via activation of AMPK may have contributed to alleviating the progression of heart failure induced by rapid RV pacing.

The second possibility is related to the improvement in insulin resistance. It is known that insulin resistance is associated with the progression of chronic heart failure, whereas chronic heart failure may provoke insulin resistance by increasing sympathetic activity, activating the renin-angiotensin system, or both.[32,33] We found that rapid RV pacing for 4 weeks induced heart failure and that metformin treatment improved insulin resistance (estimated by homeostasis model assessment–insulin resistance) compared with the pacing group, suggesting that the beneficial effect of metformin on heart failure mediated via AMPK may have been due in part to an improvement in insulin resistance.

The third possibility is the metabolic effects of AMPK activation. Both metformin and AICAR are reported to increase glucose extraction in heart,[34,35] which may decrease the severity of the failing hearts. However, we found a 2- to 3-fold increase in myocardial glucose extraction of pacing dogs, and metformin returned glucose extraction to the value of the sham group. Numerous studies have shown a switch from free fatty acids to glucose as the primary energy substrate in humans and animals with advanced heart failure,[27,36–38] suggesting that the reduction in glucose extraction by the improvement in heart failure by AMPK activation is likely to be greater than the induction of glucose extraction by direct activation of AMPK. The possibility exists that AMPK-induced glucose extraction triggers the improvement in heart failure, followed by the restoration of metabolic switch. On the other hand, we found that the net free fatty acids extraction of the pacing group tended to increase despite no statistical significance, which is consistent with the report by Paolisso et al[39] that myocardial free fatty acids extraction increased in patients with congestive heart failure[39] but is contrary to the reports of the metabolic switch.[27,36–38] The metabolic switch may differ in relatively acute or chronic heart failure and by the severity of heart failure.

The increased phosphorylation of Akt in the pacing group was attenuated in either the pacing plus metformin or the pacing plus AICAR group, suggesting that the levels of activation of insulin signaling decreased in either the

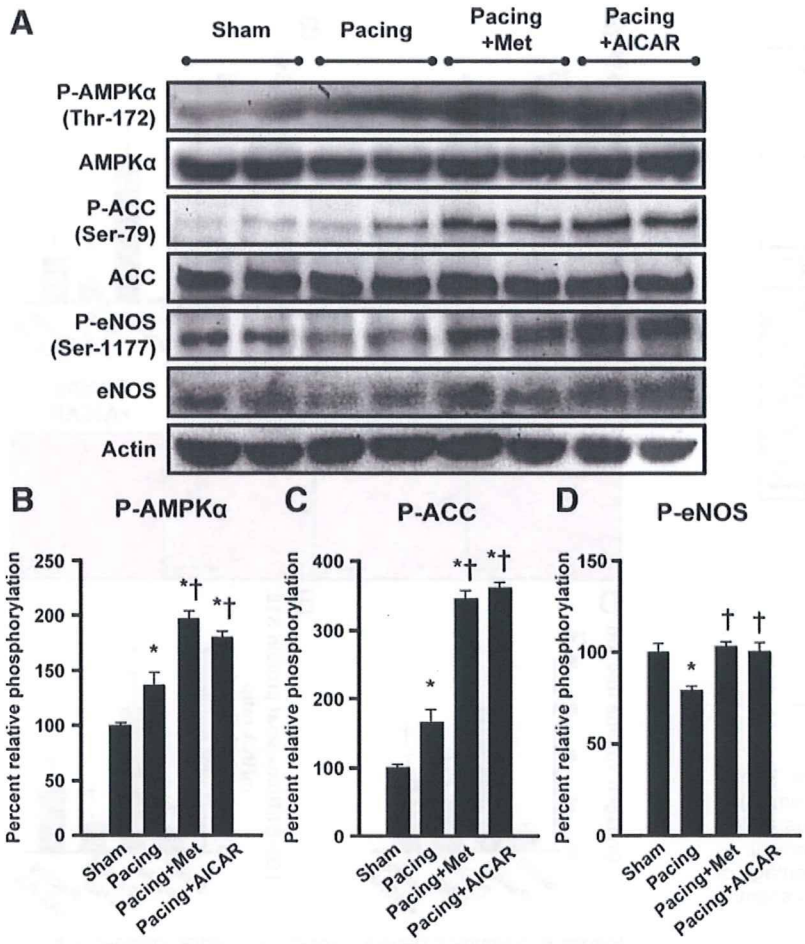

Figure 7. Phosphorylation of AMPKα, ACC, and eNOS in canine hearts after 4 weeks of treatment with or without metformin and AICAR. A, Representative immunoblots of phospho-AMPKα, ACC, and eNOS. B through D, Percentage relative phosphorylation of AMPKα, ACC, and eNOS, respectively. Values are mean±SEM. Representative results from 3 independent experiments are shown. *$P<0.05$ vs sham group; †$P<0.05$ vs pacing group.

metformin- or AICAR-treated group. Considering that glucose extraction was decreased in the pacing plus metformin and pacing plus AICAR groups and that AMPK was phosphorylated by either metformin or AICAR, which may increase in glucose extraction in the heart, the present data may be contradictory, but they are not contradictory when we consider the changes in phosphorylated Akt. The reason is that in this pacing-induced canine heart failure model, glucose extraction in the heart was influenced predominantly by insulin resistance, accompanied by the severity of heart failure, rather than AMPK phosphorylation, although further investigation on this issue is needed.

The fourth possibility is the antifibrotic effect of metformin. Several studies have indicated that AMPK activation inhibits protein synthesis through effects on both the eEF-2 and mTOR pathways.[40,41] We demonstrated that no significant difference in ventricular mass existed at autopsy among the groups. This dog pacing model has been reported to preserve wall thickness without hypertrophy or a consistent increase in heart weight, unlike the pressure overload model.[42] We found that metformin attenuated fibrosis and reduced the TGF-β1 mRNA level after 4 weeks of RV pacing compared with the pacing group. Metformin also improved representative markers of heart failure, including LV end-diastolic pressure, brain natriuretic peptide, angiotensin II, and norepinephrine. Although a number of factors may have contributed to the antifibrotic effect of metformin, our data suggest that inhibition of TGF-β1 by metformin has at least some role, resulting in the prevention of heart failure.

Taken together, these data suggest that metformin has a direct cardioprotective effect, has effects on the improvements of peripheral vascular system and insulin resistance, and inhibits fibrosis. All these actions might contribute to the improvement in the pathophysiology of heart failure, although we could not identify the exact role of each factor. It remains to be determined whether these results were a cause or consequence of improved cardiac function, especially in systemic effects of both insulin resistance and systemic vascular resistance.

Study Limitations

We found that the extent of phosphorylation of eNOS decreased despite the increase in the phosphorylated Akt in the pacing-induced failing canine hearts, which may be contradictory to previous reports that the phosphorylation of Akt leads to eNOS phosphorylation.[43,44] Because the signal transduction to modulate eNOS is unclear in the failing myocardium and the pathophysiological role and importance of Akt also are unclear, this discrepancy should be clarified in future studies.[45]

We need to consider the dose of metformin used in the present study, which was at least 3-fold higher than that used clinically. Nevertheless, adverse effects such as hypoglycemia and lactic acidosis were not detected during the experiment.

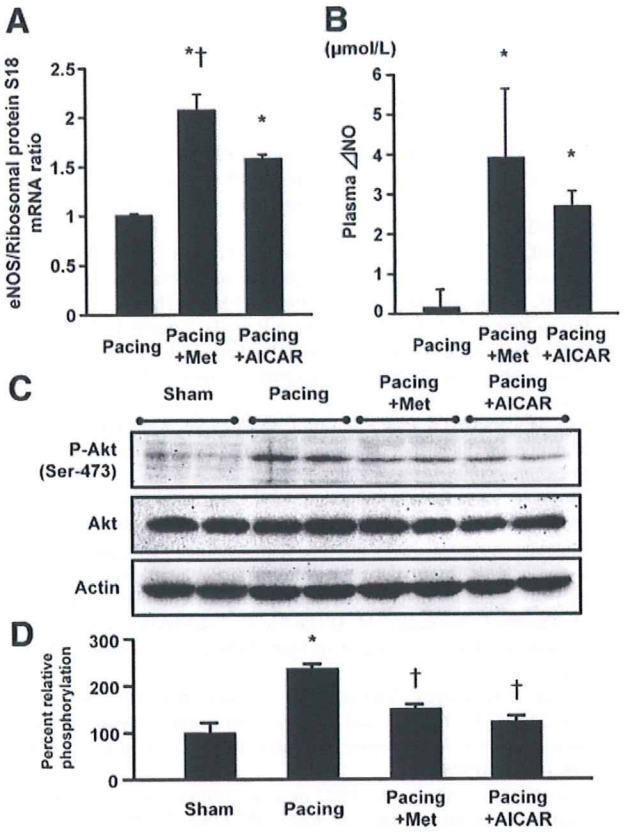

Figure 8. Effect of metformin on eNOS mRNA expression and plasma ΔNO levels, and phosphorylation of Akt in canine hearts. A, Quantitative real-time reverse-transcriptase polymerase chain reaction for eNOS mRNA. The mRNA levels were normalized to ribosomal protein S18 mRNA, and the pacing group was arbitrarily assigned a value of 1.0. B, Plasma ΔNO level after 4 weeks of RV pacing with or without metformin and AICAR administration. Values are mean±SEM. Representative results from 3 independent experiments are shown. *$P<0.05$ vs pacing group; †$P<0.05$ vs pacing plus AICAR group. C, Representative immunoblots of phospho-Akt. D, Percent relative phosphorylation of Akt. Values are mean±SEM. Representative results from 3 independent experiments are shown. *$P<0.05$ vs sham group; †$P<0.05$ vs pacing group.

Conclusions

We demonstrated that metformin prevents the progression of pacing-induced heart failure in dogs, along with the activation of AMPK. Metformin may offer a novel treatment strategy for heart failure.

Acknowledgments

We thank Yoko Horiguchi for her technical assistance; Dr Masafumi Myoishi for his assistance with TUNEL staining; Dr Hai Ying Fu for her assistance with flow cytometry; Dr Hatsue-Ishibashi-Ueda for her assistance with fluorescence microscopy; Dr Kyoko Shioya for her assistance with animal care; Tsunehisa Nakao (Nippon Shinyaku Co Ltd) for providing information about metformin; and the Evidence Finders' Club for their encouragement of this study.

Sources of Funding

This work was supported by grants in aid from the Ministry of Health, Labor, and Welfare–Japan and the Ministry of Education, Culture, Sports, Science and Technology–Japan and grants from the Japan Heart Foundation and the Japan Cardiovascular Research Foundation.

Disclosures

None.

References

1. Effect of intensive blood-glucose control with metformin on complications in overweight patients with type 2 diabetes (UKPDS 34): UK Prospective Diabetes Study (UKPDS) Group. *Lancet*. 1998;352:854–865.
2. Eurich DT, McAlister FA, Blackburn DF, Majumdar SR, Tsuyuki RT, Varney J, Johnson JA. Benefits and harms of antidiabetic agents in patients with diabetes and heart failure: systematic review. *BMJ*. 2007;335:497.
3. Zhou G, Myers R, Li Y, Chen Y, Shen X, Fenyk-Melody J, Wu M, Ventre J, Doebber T, Fujii N, Musi N, Hirshman MF, Goodyear LJ, Moller DE. Role of AMP-activated protein kinase in mechanism of metformin action. *J Clin Invest*. 2001;108:1167–1174.
4. Chan AY, Soltys CL, Young ME, Proud CG, Dyck JR. Activation of AMP-activated protein kinase inhibits protein synthesis associated with hypertrophy in the cardiac myocyte. *J Biol Chem*. 2004;279:32771–32779.
5. Zou MH, Kirkpatrick SS, Davis BJ, Nelson JS, Wiles WG 4th, Schlattner U, Neumann D, Brownlee M, Freeman MB, Goldman MH. Activation of the AMP-activated protein kinase by the anti-diabetic drug metformin in vivo: role of mitochondrial reactive nitrogen species. *J Biol Chem*. 2004;279:43940–43951.
6. Hardie DG. AMP-activated protein kinase: the guardian of cardiac energy status. *J Clin Invest*. 2004;114:465–468.
7. Calvert JW, Gundewar S, Jha S, Greer JJ, Bestermann WH, Tian R, Lefer DJ. Acute metformin therapy confers cardioprotection against myocardial infarction via AMPK-eNOS-mediated signaling. *Diabetes*. 2008;57:696–705.
8. Shibata R, Sato K, Pimentel DR, Takemura Y, Kihara S, Ohashi K, Funahashi T, Ouchi N, Walsh K. Adiponectin protects against myocardial ischemia-reperfusion injury through AMPK- and COX-2-dependent mechanisms. *Nat Med*. 2005;11:1096–1103.
9. Russell RR 3rd, Li J, Coven DL, Pypaert M, Zechner C, Palmeri M, Giordano FJ, Mu J, Birnbaum MJ, Young LH. AMP-activated protein kinase mediates ischemic glucose uptake and prevents postischemic cardiac dysfunction, apoptosis, and injury. *J Clin Invest*. 2004;114:495–503.
10. Tian R, Musi N, D'Agostino J, Hirshman MF, Goodyear LJ. Increased adenosine monophosphate-activated protein kinase activity in rat hearts with pressure-overload hypertrophy. *Circulation*. 2001;104:1664–1669.
11. Shibata R, Ouchi N, Ito M, Kihara S, Shiojima I, Pimentel DR, Kumada M, Sato K, Schiekofer S, Ohashi K, Funahashi T, Colucci WS, Walsh K. Adiponectin-mediated modulation of hypertrophic signals in the heart. *Nat Med*. 2004;10:1384–1389.
12. Liao Y, Takashima S, Maeda N, Ouchi N, Komamura K, Shimomura I, Hori M, Matsuzawa Y, Funahashi T, Kitakaze M. Exacerbation of heart failure in adiponectin-deficient mice due to impaired regulation of AMPK and glucose metabolism. *Cardiovasc Res*. 2005;67:705–713.
13. Bhalla RC, Toth KF, Tan E, Bhatty RA, Mathias E, Sharma RV. Vascular effects of metformin: possible mechanisms for its antihypertensive action in the spontaneously hypertensive rat. *Am J Hypertens*. 1996;9:570–576.
14. Marfella R, Acampora R, Verrazzo G, Ziccardi P, De Rosa N, Giunta R, Giugliano D. Metformin improves hemodynamic and rheological responses to L-arginine in NIDDM patients. *Diabetes Care*. 1996;19:934–939.
15. Katakam PV, Ujhelyi MR, Hoenig M, Miller AW. Metformin improves vascular function in insulin-resistant rats. *Hypertension*. 2000;35:108–112.
16. Rakhit RD, Marber MS. Nitric oxide: an emerging role in cardioprotection? *Heart*. 2001;86:368–372.
17. Komamura K, Shannon RP, Pasipoularides A, Ihara T, Lader AS, Patrick TA, Bishop SP, Vatner SF. Alterations in left ventricular diastolic function in conscious dogs with pacing-induced heart failure. *J Clin Invest*. 1992;89:1825–1838.
18. Lei B, Matsuo K, Labinskyy V, Sharma N, Chandler MP, Ahn A, Hintze TH, Stanley WC, Recchia FA. Exogenous nitric oxide reduces glucose transporters translocation and lactate production in ischemic myocardium in vivo. *Proc Natl Acad Sci U S A*. 2005;102:6966–6971.
19. Li HL, Yin R, Chen D, Liu D, Wang D, Yang Q, Dong YG. Long-term activation of adenosine monophosphate-activated protein kinase

attenuates pressure-overload-induced cardiac hypertrophy. *J Cell Biochem*. 2007;100:1086–1099.
20. Liao Y, Asakura M, Takashima S, Ogai A, Asano Y, Shintani Y, Minamino T, Asanuma H, Sanada S, Kim J, Kitamura S, Tomoike H, Hori M, Kitakaze M. Celiprolol, a vasodilatory beta-blocker, inhibits pressure overload-induced cardiac hypertrophy and prevents the transition to heart failure via nitric oxide-dependent mechanisms in mice. *Circulation*. 2004;110:692–699.
21. Elsner D, Riegger GA. Characteristics and clinical relevance of animal models of heart failure. *Curr Opin Cardiol*. 1995;10:253–259.
22. Lee WL, Chen JW, Ting CT, Ishiwata T, Lin SJ, Korc M, Wang PH. Insulin-like growth factor I improves cardiovascular function and suppresses apoptosis of cardiomyocytes in dilated cardiomyopathy. *Endocrinology*. 1999;140:4831–4840.
23. An D, Kewalramani G, Chan JK, Qi D, Ghosh S, Pulinilkunnil T, Abrahani A, Innis SM, Rodrigues B. Metformin influences cardiomyocyte cell death by pathways that are dependent and independent of caspase-3. *Diabetologia*. 2006;49:2174–2184.
24. Terai K, Hiramoto Y, Masaki M, Sugiyama S, Kuroda T, Hori M, Kawase I, Hirota H. AMP-activated protein kinase protects cardiomyocytes against hypoxic injury through attenuation of endoplasmic reticulum stress. *Mol Cell Biol*. 2005;25:9554–9575.
25. Mangano DT. Effects of acadesine on myocardial infarction, stroke, and death following surgery: a meta-analysis of the 5 international randomized trials: the Multicenter Study of Perioperative Ischemia (McSPI) Research Group. *JAMA*. 1997;277:325–332.
26. Kitakaze M, Takashima S, Minamino T, Node K, Shinozaki Y, Mori H, Kuzuya T, Hori M. Improvement by 5-amino-4-imidazole carboxamide riboside of the contractile dysfunction that follows brief periods of ischemia through increases in ecto-5-nucleotidase activity and adenosine release in canine hearts. *Jpn Circ J*. 1999;63:542–553.
27. Recchia FA, McConnell PI, Bernstein RD, Vogel TR, Xu X, Hintze TH. Reduced nitric oxide production and altered myocardial metabolism during the decompensation of pacing-induced heart failure in the conscious dog. *Circ Res*. 1998;83:969–979.
28. Chen ZP, Mitchelhill KI, Michell BJ, Stapleton D, Rodriguez-Crespo I, Witters LA, Power DA, Ortiz de Montellano PR, Kemp BE. AMP-activated protein kinase phosphorylation of endothelial NO synthase. *FEBS Lett*. 1999;443:285–289.
29. Zhang Y, Lee TS, Kolb EM, Sun K, Lu X, Sladek FM, Kassab GS, Garland T Jr, Shyy JY. AMP-activated protein kinase is involved in endothelial NO synthase activation in response to shear stress. *Arterioscler Thromb Vasc Biol*. 2006;26:1281–1287.
30. Davis BJ, Xie Z, Viollet B, Zou MH. Activation of the AMP-activated kinase by antidiabetes drug metformin stimulates nitric oxide synthesis in vivo by promoting the association of heat shock protein 90 and endothelial nitric oxide synthase. *Diabetes*. 2006;55:496–505.
31. Sun W, Lee TS, Zhu M, Gu C, Wang Y, Zhu Y, Shyy JY. Statins activate AMP-activated protein kinase in vitro and in vivo. *Circulation*. 2006; 114:2655–2662.
32. Swan JW, Anker SD, Walton C, Godsland IF, Clark AL, Leyva F, Stevenson JC, Coats AJ. Insulin resistance in chronic heart failure: relation to severity and etiology of heart failure. *J Am Coll Cardiol*. 1997;30:527–532.
33. Nielson C, Lange T. Blood glucose and heart failure in nondiabetic patients. *Diabetes Care*. 2005;28:607–611.
34. Fischer Y, Thomas J, Rosen P, Kammermeier H. Action of metformin on glucose transport and glucose transporter GLUT1 and GLUT4 in heart muscle cells from healthy and diabetic rats. *Endocrinology*. 1995;136: 412–420.
35. Russell RR 3rd, Bergeron R, Shulman GI, Young LH. Translocation of myocardial GLUT-4 and increased glucose uptake through activation of AMPK by AICAR. *Am J Physiol*. 1999;277:H643–H649.
36. Davila-Roman VG, Vedala G, Herrero P, de las Fuentes L, Rogers JG, Kelly DP, Gropler RJ. Altered myocardial fatty acid and glucose metabolism in idiopathic dilated cardiomyopathy. *J Am Coll Cardiol*. 2002;40: 271–277.
37. Sack MN, Rader TA, Park S, Bastin J, McCune SA, Kelly DP. Fatty acid oxidation enzyme gene expression is downregulated in the failing heart. *Circulation*. 1996;94:2837–2842.
38. Osorio JC, Stanley WC, Linke A, Castellari M, Diep QN, Panchal AR, Hintze TH, Lopaschuk GD, Recchia FA. Impaired myocardial fatty acid oxidation and reduced protein expression of retinoid X receptor-alpha in pacing-induced heart failure. *Circulation*. 2002;106:606–612.
39. Paolisso G, Gambardella A, Galzerano D, D'Amore A, Rubino P, Verza M, Teasuro P, Varricchio M, D'Onofrio F. Total-body and myocardial substrate oxidation in congestive heart failure. *Metabolism*. 1994;43: 174–179.
40. Horman S, Beauloye C, Vertommen D, Vanoverschelde JL, Hue L, Rider MH. Myocardial ischemia and increased heart work modulate the phosphorylation state of eukaryotic elongation factor-2. *J Biol Chem*. 2003; 278:41970–41976.
41. Inoki K, Zhu T, Guan KL. TSC2 mediates cellular energy response to control cell growth and survival. *Cell*. 2003;115:577–590.
42. Shinbane JS, Wood MA, Jensen DN, Ellenbogen KA, Fitzpatrick AP, Scheinman MM. Tachycardia-induced cardiomyopathy: a review of animal models and clinical studies. *J Am Coll Cardiol*. 1997;29: 709–715.
43. Montagnani M, Chen H, Barr VA, Quon MJ. Insulin-stimulated activation of eNOS is independent of Ca^{2+} but requires phosphorylation by Akt at Ser(1179). *J Biol Chem*. 2001;276:30392–30398.
44. Fulton D, Gratton JP, McCabe TJ, Fontana J, Fujio Y, Walsh K, Franke TF, Papapetropoulos A, Sessa WC. Regulation of endothelium-derived nitric oxide production by the protein kinase Akt. *Nature*. 1999;399: 597–601.
45. Shiojima I, Walsh K. Regulation of cardiac growth and coronary angiogenesis by the Akt/PKB signaling pathway. *Genes Dev*. 2006;20: 3347–3365.

CLINICAL PERSPECTIVE

Metformin is widely used as an antidiabetic drug with an insulin-sensitizing effect. A large-scale clinical trial (the UK Prospective Diabetes Study [UKPDS] 34) has shown that metformin therapy decreased the risk of cardiovascular death and the incidence of myocardial infarction associated with diabetes mellitus; metformin reduced the hemoglobin A_{1c} levels in treated patients to the same extent as in the other patients treated with conventional therapies. These results suggest that metformin might exert cardioprotective effects beyond its glucose-lowering action such as either activation of AMP-activated protein kinase (AMPK) or elevation of nitric oxide. Metformin is known to activate AMPK, which mediates potent cardioprotection against ischemia/reperfusion injury. AMPK also is activated in experimental failing myocardium, suggesting that activation of AMPK is beneficial for the pathophysiology of heart failure. The present study demonstrated that long-term oral administration of metformin prevents the progression of heart failure as indicated by hemodynamic and echocardiographic parameters. Metformin also promoted phosphorylation of both AMPK and endothelial nitric oxide synthase, increased plasma nitric oxide levels, and improved insulin resistance. As a result of these effects, metformin decreased apoptosis and improved cardiac function in failing canine hearts. Interestingly, another AMPK activator (AICAR) had effects equivalent to those of metformin, suggesting the primary role of AMPK activation in reducing apoptosis and preventing heart failure. Drugs that activate AMPK, especially metformin, may provide a novel strategy for the treatment of heart failure in clinical settings.

Supplemental Methods

The animal experiments were approved by the National Cardiovascular Center Research Committee and were performed according to institutional guidelines.

Experimental Protocols

1) Effects of Metformin on Cardiomyocyte Viability and Apoptosis After Exposure to H_2O_2

To investigate whether metformin has a cardioprotective effect against damage due to H_2O_2 in vitro, we assessed cell viability and apoptosis in cultured cardiomyocytes using the 3-(4,5-dimethylthiazol-2-yl)-2,5-diphenyl tetrazolium bromide (MTT) assay and both the terminal deoxynucleotidyl transferase-mediated dUTP nick-end labeling (TUNEL) staining plus flow cytometry, respectively. The cells were cultured in serum-free media for 24 hours and then incubated in the presence of 50 μmol/L H_2O_2 for 24 hours. Cardiomyocytes were pretreated with either metformin (1 to 100 μmol/L) or 5-amino-4-imidazole-1-β-D-carboxamide ribofuranoside (AICAR; an AMPK activator) (500 μmol/L) for 60 minutes before the addition of H_2O_2. Other cells were preincubated with an AMPK inhibitor, compound-C (20 μmol/L) for 6 hours before the addition of either metformin or AICAR. Then cell viability and apoptosis were analyzed.

2) Effects of Metformin on Cardiac Performance in Dogs With Pacing-Induced Heart Failure

After pacemaker implantation, the dogs were randomly assigned to 3 groups as follows: 1) a group that received a normal diet and drinking water (Pacing group, n=8), 2) a group that received metformin orally at a dose of 100 mg/kg/day (Pacing+Met group, n=8), and 3) a group received AICAR

subcutaneously every other day at 5 mg/kg (Pacing+AICAR group, n=4). We also performed a sham operation in another 6 dogs (Sham group, n=6). The dose of metformin (100 mg/kg/day) was selected because our preliminary study showed that this was the maximum dose that did not induce hypoglycemia (data not shown). The dose of AICAR (5 mg/kg subcutaneously on alternate days) was selected because we preliminarily confirmed that phosphorylation of AMPK was elevated at least 48 hours after subcutaneous injection of AICAR, by reference to previous report in rats, due to the lack of any data for dogs (Supplemental Figures).[1] Echocardiography was performed and hemodynamic parameters were measured before and after 4 weeks of right ventricular (RV) pacing. After assessment of these parameters, each heart was excised and divided into three parts for immunoblotting, quantitative reverse-transcriptase polymerase chain reaction (PCR), and histological examination.

Materials

1, 1-Dimethylbiguanide hydrochloride (metformin hydrochloride) was a kind gift from Nippon Shinyaku Co. Ltd. (Kyoto, Japan), while AICAR (an AMPK activator) and compound-C (an AMPK inhibitor) were purchased from Calbiochem (California, USA). Antibodies directed against endothelial nitric oxide synthase (eNOS) were obtained from Affinity BioReagents (Colorado, USA). Other antibodies were purchased from Cell Signaling Technology (Massachusetts, USA).

Cell Culture

Primary cultures of cardiomyocytes were prepared from ventricles of 1-day-old Wistar rats, as described previously.[2] In brief, cardiomyocytes were plated at a density of 5×10^5 cells/mL on

collagen-coated culture dishes and incubated in standard medium (DMEM with 10% FBS) for 72 hours, after which incubation was continued under serum-free conditions for 48 hours.

Cell Viability Assay (MTT Assay)

Cell viability was analyzed by a nonradioactive cell proliferation assay using MTT, as described previously with minor modifications[3].

Assessment of Cardiomyocyte Apoptosis

To investigate the influence of metformin on cardiomyocyte viability, TUNEL assay was performed as reported previously.[3] Apoptosis was also quantified by flow cytometry (FACScan; Becton, Dickinson and Company, New Jersey, USA) after cells were stained with annexin V and propidine iodide (PI) according to the manufacturer's instructions (Annexin V-FITC Apoptosis Detection Kit; Sigma, Saint Louis, USA).

Canine Pacing Model

Beagle dogs (Oriental Yeast Co. Ltd, Tokyo, Japan) weighing 8 to 10 kg were sedated with intravenous sodium pentobarbital at a dose of 25 mg/kg. After intubation with a cuffed endotracheal tube, anesthesia was maintained with 0.5 % to 1% isoflurane and an equal mixture of air and oxygen. Ventilation was provided with a tidal volume of 22 mL/kg at a rate of 15 times per minute. A bipolar pacing lead (Model BT-45P, Star Medical Inc., Tokyo, Japan) was advanced under fluoroscopic guidance through the right jugular vein to the RV apex and was connected to a programmable pacemaker (VOO mode; Model SIP-501, Star Medical Inc., Tokyo, Japan) that was implanted in a

subcutaneous pocket in the neck. The success of this procedure was confirmed by electrocardiography. Cefazolin sodium (1 g) was given intravenously after surgery, and the dogs were allowed to recover for a few hours. Then heart failure was induced by rapid RV pacing at a rate of 230 beats per minute for 4 weeks, as reported previously.[4]

Echocardiography

Transthoracic echocardiography was performed by using an echocardiographic system equipped with a 4-MHz phased-array transducer (SONOS 5500, PHILIPS, Eindhoven, the Netherlands) in conscious dogs before pacemaker implantation and 30 minutes after the cessation of right ventricular (RV) pacing at 4 weeks. A two-dimensional short-axis view of the left ventricle was obtained at the level of the papillary muscles. All measurements were made by two observers, who were blinded with respect to the source of the tracings.

Hemodynamic Studies

Both left ventricular end-diastolic pressure (LVEDP) and mean aortic pressure were measured by pressure transducers using a 5 Fr pig tail catheter (Terumo Co. Ltd., Tokyo, Japan) that was inserted into the left ventricle from the left femoral artery. The mean pulmonary artery pressure (PAP) and the pulmonary capillary wedge pressure (PCWP) were measured using a 7 Fr Swan-Ganz catheter (American Edwards Laboratories, California, USA). Cardiac output (CO) was determined at least three times by the thermodilution technique. Systemic vascular resistance (SVR) was calculated as follows: (mean aortic pressure-right atrial pressure) × 80/CO.

Histological examination

The collagen volume fraction was examined in sections of the left ventricular (LV) free wall, after excluding vessels, artifacts, minor scars, and incomplete tissue. Specimens were stained with Masson's trichrome stain to evaluate the extent of interstitial fibrosis, as described previously.[5] The area of stained tissue was calculated as a percentage of the total area within a field by using Scion image software (Beta 4.0.2).

Quantitative Reverse-Transcriptase PCR

The quantitative reverse-transcriptase PCR was performed as described previously.[6] Total RNA was extracted from LV myocardium with RNA-Bee-RNA Isolation Reagent (Tel-Test, Texas, USA). Then 1,000 ng of total RNA was reverse transcribed and amplified with an Omniscript RT Kit (Qiagen, Hilden, Germany) according to the manufacturer's protocol.

Oligonucleotide primers and TaqMan probes for canine atrial natriuretic peptide (ANP) (Cf 02705687_g1), canine transforming growth factor-β1 (TGF-β1) (Cf 02741608_m1), and canine ribosomal protein S18 (Cf 02681523_g1) were purchased from Applied Biosystems (California, USA). Both Taqman probe and primer designs were optimized to enhance stability on the basis of the known sequences of canine brain natriuretic peptide (BNP)[7] and canine endothelial NO synthase (eNOS).[8] We used the following probes, sense primers, and antisense primers: 5'-FAM-CAGTTGGCCCTGGAA-MGB-3', 5'-GAAGGACGCAGTTTCAGAGCTG -3' and 5'-AAAGCACCCTGACTTGTGCATC-3' for canine BNP; and

5'-FAM-CCTGGAGGATGTGGC-MGB-3', 5'-AACCTGTGTGACCCTCATCGAT-3' and 5'-TCACTTTGGCCAGCTGGTAACT-3' for canine eNOS, respectively.

Immunoblotting

Immunoblotting was performed as described previously.[9] A Bio-Rad ChemiDoc XRS system (Bio-Rad Laboratories, Inc., California, USA) was used for chemiluminescence imaging and immunoreactive bands were quantified with Bio-Rad Quantity One 1-D analysis software (Bio-Rad Laboratories, Inc., California, USA).

Measurement of Nitric Oxide End-Products

The plasma level of nitric oxide (NO) metabolic end-products (nitrite + nitrate) was measured by the Griess method, as reported previously.[10] Subsequently, ΔNO was defined as the difference between the plasma NO level before and after 4 weeks of RV pacing.

Metabolic Parameters

All dogs were fed a standard diet with a fixed carbohydrate and fat content (DS-A, Oriental Yeast Co. Ltd, Tokyo, Japan). After fasting for 14 hours, metabolic parameters such as the plasma levels of glucose, lactate, free fatty acids (FFA), and insulin were measured with a quick-auto-neo-GLU-HK (Shino-Test Corporation, Tokyo, Japan.), Determiner LA (KYOWA MEDEX Co., Ltd., Tokyo, Japan.), NEFA-SS Eiken, Eiken Chemical Co., Ltd., Tokyo, Japan.), and YK060 Insulin ELISA Kit (Yanaihara Institute Inc. Shizuoka, Japan), respectively. Insulin resistance was assessed from the fasting insulin and glucose levels by the homeostasis model assessment-insulin resistance (HOMA-IR) method, i.e.,

HOMA-IR is [fasting glucose (mmol/L) × fasting insulin (μU/mL)] / 22.5.[11] The levels of norepinephrine and angiotensin II were measured by using a CA test TOSOH (Tosoh Corporation, Tokyo, Japan.) and a NEX-105 (125I)-Tyr4-Angiotensin II test (PerkinElmer Inc., Massachusetts, USA.), respectively. Myocardial substrate extraction was calculated as described previously.[12]

Measurement of Body Fat and Activity in Dogs

To examine the effects of metformin on body fat and physical activity in this dog model of pacing-induced heart failure, we measured body fat with a dog body fat counter (IBF-D02, Kao Corporation, Tokyo, Japan) and evaluated physical activity by using a pedometer (SE-MG10, SATO KEIRYOUKI MFG. Co., Ltd., Tokyo, Japan) attached to each dog's collar.

Supplemental Figures

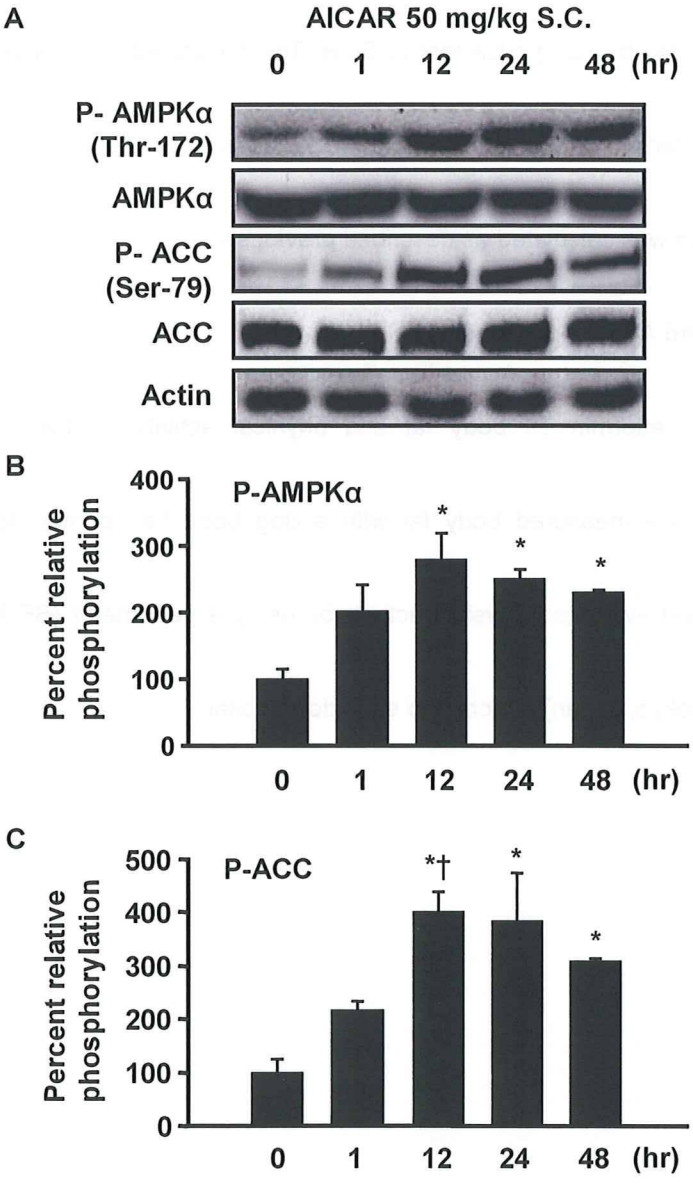

Changes in the phosphorylation of AMPKα and ACC in canine hearts after subcutaneous administration of AICAR. A) Representative immunoblots of phospho-AMPKα and ACC. **B)** and **C)** The percent relative phosphorylation of AMPKα and ACC, respectively. Values are the mean±SEM. *P<0.05 vs. no treatment; †P<0.05 vs. one hour after subcutaneous administration of AICAR. Representative results from 3 independent experiments are shown.

Supplemental References :

1. Li HL, Yin R, Chen D, Liu D, Wang D, Yang Q, Dong YG. Long-term activation of adenosine monophosphate-activated protein kinase attenuates pressure-overload-induced cardiac hypertrophy. *J Cell Biochem.* 2007;100:1086-1099.

2. Asakura M, Kitakaze M, Takashima S, Liao Y, Ishikura F, Yoshinaka T, Ohmoto H, Node K, Yoshino K, Ishiguro H, Asanuma H, Sanada S, Matsumura Y, Takeda H, Beppu S, Tada M, Hori M, Higashiyama S. Cardiac hypertrophy is inhibited by antagonism of ADAM12 processing of HB-EGF: metalloproteinase inhibitors as a new therapy. *Nat Med.* 2002;8:35-40.

3. Okada K, Minamino T, Tsukamoto Y, Liao Y, Tsukamoto O, Takashima S, Hirata A, Fujita M, Nagamachi Y, Nakatani T, Yutani C, Ozawa K, Ogawa S, Tomoike H, Hori M, Kitakaze M. Prolonged endoplasmic reticulum stress in hypertrophic and failing heart after aortic constriction: possible contribution of endoplasmic reticulum stress to cardiac myocyte apoptosis. *Circulation.* 2004;110:705-712.

4. Shinbane JS, Wood MA, Jensen DN, Ellenbogen KA, Fitzpatrick AP, Scheinman MM. Tachycardia-induced cardiomyopathy: a review of animal models and clinical studies. *J Am Coll Cardiol.* 1997;29:709-715.

5. Wakeno M, Minamino T, Seguchi O, Okazaki H, Tsukamoto O, Okada K, Hirata A, Fujita M, Asanuma H, Kim J, Komamura K, Takashima S, Mochizuki N, Kitakaze M. Long-term stimulation of adenosine A2b receptors begun after myocardial infarction prevents cardiac

remodeling in rats. *Circulation.* 2006;114:1923-1932.

6. Fujita M, Okuda H, Tsukamoto O, Asano Y, Hirata YL, Kim J, Miyatsuka T, Takashima S, Minamino T, Tomoike H, Kitakaze M. Blockade of angiotensin II receptors reduces the expression of receptors for advanced glycation end products in human endothelial cells. *Arterioscler Thromb Vasc Biol.* 2006;26:e138-142.

7. Lisy O, Redfield MM, Schirger JA, Burnett JC, Jr. Atrial BNP endocrine function during chronic unloading of the normal canine heart. *Am J Physiol Regul Integr Comp Physiol.* 2005;288:R158-162.

8. Fulton D, Papapetropoulos A, Zhang X, Catravas JD, Hintze TH, Sessa WC. Quantification of eNOS mRNA in the canine cardiac vasculature by competitive PCR. *Am J Physiol Heart Circ Physiol.* 2000;278:H658-665.

9. Tsukamoto O, Minamino T, Okada K, Shintani Y, Takashima S, Kato H, Liao Y, Okazaki H, Asai M, Hirata A, Fujita M, Asano Y, Yamazaki S, Asanuma H, Hori M, Kitakaze M. Depression of proteasome activities during the progression of cardiac dysfunction in pressure-overloaded heart of mice. *Biochem Biophys Res Commun.* 2006;340:1125-1133.

10. Asanuma H, Node K, Minamino T, Sanada S, Takashima S, Ueda Y, Sakata Y, Asakura M, Kim J, Ogita H, Tada M, Hori M, Kitakaze M. Celiprolol increases coronary blood flow and reduces severity of myocardial ischemia via nitric oxide release. *J Cardiovasc Pharmacol.* 2003;41:499-505.

11. Bonora E, Targher G, Alberiche M, Bonadonna RC, Saggiani F, Zenere MB, Monauni T, Muggeo M. Homeostasis model assessment closely mirrors the glucose clamp technique in the assessment of insulin sensitivity: studies in subjects with various degrees of glucose tolerance and insulin sensitivity. *Diabetes Care.* 2000;23:57-63.

12. Nikolaidis LA, Elahi D, Hentosz T, Doverspike A, Huerbin R, Zourelias L, Stolarski C, Shen YT, Shannon RP. Recombinant glucagon-like peptide-1 increases myocardial glucose uptake and improves left ventricular performance in conscious dogs with pacing-induced dilated cardiomyopathy. *Circulation.* 2004;110:955-961.

Autonomic Neuroscience: Basic and Clinical 148 (2009) 44–49

Contents lists available at ScienceDirect

Autonomic Neuroscience: Basic and Clinical

journal homepage: www.elsevier.com/locate/autneu

In vivo direct monitoring of vagal acetylcholine release to the sinoatrial node

Shuji Shimizu [a,c,d,*], Tsuyoshi Akiyama [b], Toru Kawada [a], Toshiaki Shishido [a], Toji Yamazaki [b], Atsunori Kamiya [a], Masaki Mizuno [a], Shunji Sano [c], Masaru Sugimachi [a]

[a] Department of Cardiovascular Dynamics, Advanced Medical Engineering Center, National Cardiovascular Center Research Institute, Osaka, Japan
[b] Department of Cardiac Physiology, National Cardiovascular Center Research Institute, Osaka, Japan
[c] Department of Cardiovascular Surgery, Okayama University Graduate School of Medicine, Dentistry and Pharmaceutical Sciences, Okayama, Japan
[d] Japan Association for the Advancement of Medical Equipment, Tokyo, Japan

ARTICLE INFO

Article history:
Received 30 September 2008
Received in revised form 16 February 2009
Accepted 23 February 2009

Keywords:
Heart rate
Vagal nerve activity
Acetylcholine
Sinoatrial node
Right atrium
Microdialysis
Anesthetized rabbit

ABSTRACT

To directly monitor vagal acetylcholine (ACh) release into the sinoatrial node, which regulates heart rate, we implanted a microdialysis probe in the right atrium near the sinoatrial node and in the right ventricle of anesthetized rabbits, and perfused with Ringer's solution containing eserine. (1) Electrical stimulation of right or left cervical vagal nerve decreased atrial rate and increased dialysate ACh concentration in the right atrium in a frequency-dependent manner. Compared to left vagal stimulation, right vagal nerve stimulation decreased atrial rate to a greater extent at all frequencies, and increased dialysate ACh concentration to a greater extent at 10 and 20 Hz. However, dialysate ACh concentration in the right atrium correlated well with atrial rate independent of whether electrical stimulation was applied to the right or left vagal nerve (atrial rate $= 304 - 131 \times \log[\mathrm{ACh}]$, $R^2 = 0.77$). (2) Right or left vagal nerve stimulation at 20 Hz decreased atrial rate and increased dialysate ACh concentrations in both the right atrium (right, 17.9 ± 4.0 nM; left, 7.9 ± 1.4 nM) and right ventricle (right, 0.9 ± 0.3 nM; left, 1.0 ± 0.4 nM). However, atrial dialysate ACh concentrations were significantly higher than ventricular concentrations, while ventricular dialysate ACh concentrations were not significantly different between right and left vagal nerve stimulation. (3) The response of ACh release to right and left vagal nerve stimulation was abolished by intravenous administration of a ganglionic blocker, hexamethonium bromide. In conclusion, ACh concentration in dialysate from the right atrium, sampled by microdialysis, is a good marker of ACh release from postganglionic vagal nerves to the sinoatrial node.

1. Introduction

Parasympathetic nerves play an important role in the regulation of heart rate under physiological conditions. To better understand the parasympathetic control of heart rate, it is important to quantitatively assess the efferent cardiac vagal nerve activity. Several methods have been used to assess this activity. Efferent cardiac vagal nerve electrical activity has been measured directly at the preganglionic site in several studies (Jewett, 1964; Kunze, 1972). We have developed a microdialysis technique which is used with high-performance liquid chromatography (HPLC) to monitor in vivo endogenous acetylcholine (ACh) release in the heart (Akiyama et al., 1994). Using this technique, we were able to monitor endogenous ACh release into the ventricular myocardium (Akiyama et al., 1994; Kawada et al., 2001). This technique permits the estimation of relative changes in postganglionic efferent cardiac vagal nerve activity in the ventricle.

However, vagal innervation is known to be heterogeneous in the heart. Kilbinger and Löffelholz (1976) reported that the ACh content of the ventricle was 41% and 19% of the atrial content in chicken and rabbit, respectively. Brown (1976) reported that ACh concentration was higher in the atrium than the ventricle, and that ACh content was higher in the right than the left portions in both the atrium and ventricle of the cat. Thus, to better understand the parasympathetic control of heart rate, which is the sinus rate under physiological conditions, we need information about the activities of postganglionic vagal nerves innervating the sinoatrial (SA) node.

In this study, we developed a dialysis probe using shorter dialysis fiber, which was suitable for implantation into the atrium. Using this dialysis probe, we tried to monitor myocardial interstitial ACh levels in the right atrium, especially near the SA node. Furthermore, we investigated whether the myocardial interstitial ACh levels reflect relative changes in activity of postganglionic vagal nerves innervating the SA node.

2. Materials and methods

2.1. Surgical preparation

Animal care was provided in accordance with the *Guiding Principles for the Care and Use of Animals in the Field of Physiological Sciences*

* Corresponding author. Department of Cardiovascular Dynamics, Advanced Medical Engineering Center, National Cardiovascular Center Research Institute, 5-7-1, Fujishiro-dai, Suita, Osaka, 565-8565 Japan. Tel.: +81 6 6833 5012; fax: +81 6 6835 5403.
E-mail address: shujismz@ri.ncvc.go.jp (S. Shimizu).

1566-0702/$ – see front matter © 2009 Elsevier B.V. All rights reserved.
doi:10.1016/j.autneu.2009.02.006

approved by the Physiological Society of Japan. All protocols were approved by the Animal Subject Committee of the National Cardiovascular Center. Forty-three Japanese white rabbits weighing from 2.2 to 2.9 kg were anesthetized using an intravenous injection of pentobarbital sodium (50 mg/kg) via the marginal ear vein, followed by a continuous intravenous infusion of α-chloralose and urethane (16 mg/kg/h and 100 mg/kg/h) through a catheter inserted into the femoral vein to maintain an appropriate level of anesthesia. The animals were intubated and ventilated mechanically with room air mixed with oxygen. Systemic arterial pressure was monitored by a catheter inserted into the femoral artery. Esophageal temperature, which was measured by a thermometer (CTM-303, TERUMO, Japan), was maintained between 38 and 39 °C using a heating pad. In all protocols, bilateral vagal nerves were exposed through a midline cervical incision and sectioned at the neck after the control dialysate sampling. A pair of bipolar stainless steel electrodes was attached to the efferent side of the right or left vagal nerve. The nerve and electrode were covered with warmed mineral oil for insulation. When vagal stimulation was required, the efferent vagal nerve was stimulated by a digital stimulator (SEN-7203, Nihon Kohden, Japan). The pulse duration and amplitude of nerve stimulation were set at 1 ms and 10 V.

With the animal in the lateral position, right lateral thoracotomy was performed and the right 3rd to 5th ribs were partially resected to expose the heart. After incision of the pericardium, stainless steel wires were attached to the apex and the anterior wall of the left ventricle for ventricular pacing. To prevent severe bradycardia and cardiac arrest induced by vagal stimulation, left ventricular pacing was performed at the same frequency as the heart rate before vagal stimulation. The ventricular rate was determined from the electrocardiogram using a cardiotachometer. Another pair of stainless steel wires was attached to the appendage of the right atrium for recording atrial electrocardiogram, from which atrial rate was determined. Heparin sodium (100 IU/kg) was administered intravenously to prevent blood coagulation. At the end of the experiment, animals were killed with an overdose injection of pentobarbital sodium. A postmortem examination confirmed that the dialysate probe did not penetrate into the atrial or ventricular cavity and the dialysis membrane was positioned totally within the atrial or ventricular wall.

2.2. Dialysis technique

The materials and properties of the dialysis probe have been described previously (Akiyama et al., 1994). Briefly, we designed a handmade transverse dialysis probe. A dialysis fiber of semipermeable membrane (4 mm length, 310 μm outer diameter, 200 μm inner diameter; PAN-1200, 50,000 molecular weight cutoff; Asahi Chemical, Tokyo, Japan) was attached at both ends to polyethylene tubes (25 cm length, 500 μm outer diameter, 200 μm inner diameter). A fine guiding needle (30 mm length, 510 μm outer diameter, 250 μm inner diameter) with a stainless steel rod (5 mm length, 250 μm outer diameter) was used for the implantation of the dialysis probe. In protocol 1 and 3, a dialysis probe was implanted in the right atrium near the junction between the superior vena cava and the right atrium. In protocol 2, a dialysis probe was also implanted in the right ventricular free wall. After implantation, the dialysis probe was perfused with Ringer's solution (NaCl 147 mM, KCl 4 mM, $CaCl_2$ 3 mM) containing the cholinesterase inhibitor eserine (100 μM) at a speed of 2 μl/min, using a microinjection pump (CMA/100, Carnegie Medicin, Sweden). Experimental protocols were started 120 min after implantation of the dialysis probe. We took account of the dead space between the dialysis membrane and the sample tube at the start of each dialysate sampling. Phosphate buffer (4 μl) containing an internal standard (isopropylhomocholine chloride) was transferred into each sample tube before dialysate sampling. Dialysate sampling periods were set at 10 min (1 sample volume = 20 μl).

2.3. Analytic procedure

Dialysate ACh was assayed using HPLC with electrochemical detection. An autosampler (CMA/200, Carnegie Medicin) was used. The HPLC system consisted of a pump with a pulse dumper (EP-300, Eicom, Japan), a separation column (AC-Gel, styrene polymer, 4 μm particle size, 2 mm inner diameter × 150 mm length, Eicom), an immobilized enzyme column (AC-Enzymepack, 1 mm inner diameter × 4 mm length, Eicom), an electrochemical detector (ECD-300, Eicom), and a degasser (DG-300, Eicom). The electrochemical detector was operated with a platinum working electrode at + 0.45 V vs. an Ag/AgCl reference electrode. The mobile phase was 50 mM potassium bicarbonate solution containing 400 mg/L of sodium 1-decansulfonate and 50 mg/L of disodium-EDTA. The pump flow rate was 0.15 ml/min.

Chromatograms were recorded and analyzed by an analog-to-digital converter (Power Chrom EPC-300, AD Instruments, Australia) with a computer. Concentrations of ACh and isopropylhomocholine chloride were determined by measuring the peak areas. The absolute detection limit of ACh was 10 fmol/injection (signal-to-noise ratio = 3).

2.4. Experimental protocols

2.4.1. Protocol 1

To examine whether atrial dialysate ACh concentration reflects ACh release from cardiac vagal nerves, we investigated the relationship between the dialysate ACh concentration in the right atrium and the frequency of right and left vagal nerve stimulation. We sampled control dialysate before and after vagal transection. Then we stimulated the right ($n = 8$) or left ($n = 8$) efferent vagal nerves for 10 min at frequencies of 5, 10, 20 and 40 Hz, and sampled dialysate during each stimulation. Ten minutes after vagal nerve stimulation, we sampled the dialysate again to check the recovery of ACh levels.

2.4.2. Protocol 2

To investigate the difference in vagal innervation density between the right atrium and right ventricle, we compared the atrial and ventricular dialysate ACh concentrations under control condition and during electrical vagal nerve stimulation. Control dialysates were sampled after vagal transection. Then the right ($n = 5$) or left ($n = 5$) efferent vagal nerve was stimulated for 10 min at a frequency of 20 Hz, and dialysates were collected during vagal stimulation.

2.4.3. Protocol 3

ACh is released from both pre- and post-ganglionic vagal nerves as a primary neurotransmitter. The cardiac vagal nerve ganglia are localized near the atrium (Löffelholz and Pappano, 1985). Electrical stimulation of cervical vagal nerves activates the entire efferent parasympathetic pathway, including both preganglionic and postganglionic nerves in the atrium. Thus it is possible that pre- and/or post-ganglionic nerves serve as the source of dialysate ACh. To determine whether pre- or post-ganglionic nerves are the source of atrial dialysate ACh, we observed ACh release in response to nerve stimulation before and after blockade of ganglionic transmission. We sampled control dialysate after vagal transection. Then we stimulated the right ($n = 9$) or left ($n = 8$) vagal nerve at a frequency of 20 Hz before and after intravenous administration of hexamethonium bromide (30 mg/kg) and sampled dialysate during vagal stimulation. To prevent severe hypotension induced by hexamethonium, arterial pressure was maintained by continuous intravenous infusion of phenylephrine (17.2 ± 1.6 μg/kg/min).

2.5. Statistical analysis

All data are presented as mean ± SE. For each protocol, heart rate and mean arterial pressure were compared by one-way repeated measures analysis of variance followed by a Dunnett's test against

control (Glantz, 2005). In protocol 1, we compared vagal stimulation-induced ACh release among the seven groups by one-way repeated measures analysis of variance followed by Tukey's test. Heart rates (atrial rate) and dialysate ACh concentrations during right and left vagal stimulation were compared by unpaired *t*-test. After logarithmic transformation of atrial dialysate ACh concentration, a linear regression analysis was performed to examine the relation between dialysate ACh concentration and atrial rate. In protocol 2, we compared atrial and ventricular dialysate ACh concentrations during vagal stimulation by two-way repeated measures analysis of variance. We also compared the effects of right and left vagal stimulation on atrial and ventricular dialysate ACh concentrations using an unpaired *t*-test. In protocol 3, we compared stimulation-induced ACh release with and without hexamethonium using one-way repeated measures analysis of variance followed by a Dunnett's test against control. Differences were considered significant at $P<0.05$.

3. Results

3.1. Protocol 1

Responses of heart rate and mean arterial pressure to electrical vagal nerve stimulation are shown in Table 1. Transection of bilateral vagal nerves did not change heart rate or mean arterial pressure significantly. While both right and left vagal stimulation decreased heart rate in proportion to the frequency of the stimulus, right vagal nerve stimulation decreased the heart rate to a greater extent than left vagal nerve stimulation at all stimulus frequencies tested ($P<0.05$ at 5 Hz, $P<0.01$ at 10 Hz, $P<0.05$ at 20 Hz and $P<0.05$ at 40 Hz). Heart rate recovered to the pre-stimulation levels after stimulation. Both right and left vagal nerve stimulation with ventricular pacing decreased mean arterial pressure. Mean arterial pressure recovered partially but remained lower than the pre-stimulation levels 10 min after stimulation.

Transection of bilateral vagal nerves did not change dialysate ACh concentration (Fig. 1). Both right and left vagal stimulation increased the dialysate ACh concentration in proportion to the stimulus frequency. Right vagal stimulation increased the dialysate ACh concentration from 1.9 ± 0.3 nM in the post-transection control to 2.7 ± 0.4 nM at 5 Hz ($P<0.05$ vs. control), 5.5 ± 0.8 nM at 10 Hz ($P<0.01$ vs. 5 Hz), 17.2 ± 3.0 nM at 20 Hz ($P<0.01$ vs. 10 Hz) and 40.4 ± 8.4 nM at 40 Hz ($P<0.01$ vs. 20 Hz). Dialysate ACh concentration recovered to 2.2 ± 0.3 nM 10 min after stimulation. Left vagal stimulation increased dialysate ACh concentration from 1.6 ± 0.3 nM in the post-transection control to 2.2 ± 0.4 nM at 5 Hz (N.S. vs. control), 3.2 ± 0.5 nM at 10 Hz ($P<0.01$ vs. control), 8.2 ± 1.4 nM at 20 Hz ($P<0.01$ vs. 10 Hz) and 24.7 ± 4.6 nM at 40 Hz ($P<0.01$ vs. 20 Hz). Dialysate ACh concentration recovered to 2.0 ± 0.5 nM 10 min after stimulation. While both right and left vagal stimulation increased dialysate ACh concentration in a frequency-dependent manner, right vagal nerve stimulation increased dialysate ACh concentration to a greater extent than left vagal nerve stimulation at 10 and 20 Hz (N.S. at 5 Hz, $P<0.05$ at 10 Hz, $P<0.05$ at 20 Hz and N.S. at 40 Hz).

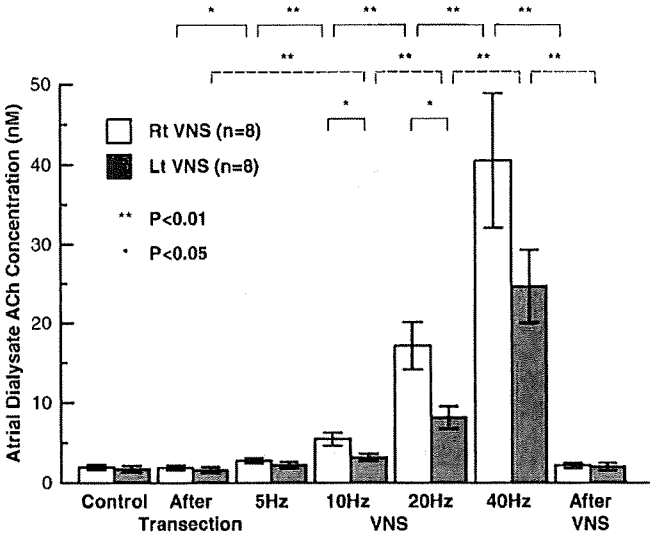

Fig. 1. Dialysate ACh concentrations of controls and during electrical vagal nerve stimulation at different frequencies. Right vagal nerve stimulation increased atrial dialysate ACh concentration from 1.9 ± 0.3 nM in the post-transection control to 2.7 ± 0.4 nM at 5 Hz, 5.5 ± 0.8 nM at 10 Hz, 17.2 ± 3.0 nM at 20 Hz and 40.4 ± 8.4 nM at 40 Hz. Left vagal nerve stimulation increased atrial dialysate ACh concentration from 1.6 ± 0.3 nM in the control to 2.2 ± 0.4 nM at 5 Hz, 3.2 ± 0.5 nM at 10 Hz, 8.2 ± 1.4 nM at 20 Hz and 24.7 ± 4.6 nM at 40 Hz. Values are means ± SE; Rt: right; Lt: left; VNS: electrical vagal nerve stimulation; *n*: number of rabbits: $^{**}P<0.01$, $^{*}P<0.05$.

The relationship between dialysate ACh concentration and atrial rate ($n=16$) is shown in Fig. 2. Dialysate ACh concentration in the right atrium correlated well with atrial rate (AR; $AR=304-131\times\log[ACh]$, $R^2=0.77$). There was no significant difference in the intercept or slope of regression line between right and left vagal nerve stimulation (right: $AR=304-135\times\log[ACh]$, $R^2=0.79$; left: $AR=303-126\times\log[ACh]$, $R^2=0.73$) (Glantz, 2005). The correlation between dialysate ACh concentration and atrial rate was independent of the side of vagal nerve stimulation.

Table 1
Responses of heart rate and mean arterial pressure to electrical vagal nerve stimulation (protocol 1).

	Heart rate (bpm)	Mean arterial pressure (mm Hg)
Rt vagal stimulation ($n=8$)	Atrial rate (pacing rate)	
Control before transection	298 ± 8	83 ± 4
Control after transection	293 ± 7	85 ± 6
VNS (5 Hz)	246 ± 5** (296 ± 5)	71 ± 7
VNS (10 Hz)	201 ± 6** (296 ± 5)	77 ± 6
VNS (20 Hz)	121 ± 7** (296 ± 5)	72 ± 8
VNS (40 Hz)	88 ± 4** (296 ± 5)	65 ± 7**
After VNS	287 ± 10	70 ± 9
Lt vagal stimulation ($n=8$)	Atrial rate (pacing rate)	
Control before transection	305 ± 8	89 ± 4
Control after transection	308 ± 5	92 ± 6
VNS (5 Hz)	267 ± 6* (309 ± 4)	79 ± 6**
VNS (10 Hz)	236 ± 10** (309 ± 4)	82 ± 6
VNS (20 Hz)	165 ± 13** (309 ± 4)	77 ± 5**
VNS (40 Hz)	129 ± 16** (309 ± 4)	67 ± 6**
After VNS	305 ± 13	75 ± 8**

Values are means ± SE; *n*: numbers of rabbits; Rt: right; Lt: left; VNS: electrical vagal nerve stimulation; $^{**}P<0.01$ vs. control; $^{*}P<0.05$ vs. control.

3.2. Protocol 2

Responses of heart rate and mean arterial pressure were similar to the responses to vagal stimulation at 20 Hz in protocol 1 (Table 2). Responses of ACh release in the right atrium and right ventricle to vagal stimulation are shown in Fig. 3. Right vagal stimulation increased the atrial dialysate ACh concentration from 2.6 ± 0.6 nM in the post-transection control to 17.9 ± 4.0 nM ($P<0.01$) and the ventricular dialysate ACh concentration from 0.4 ± 0.2 nM to 0.9 ± 0.3 nM ($P<0.01$). Left vagal stimulation also increased the atrial dialysate ACh concentration from 1.5 ± 0.4 nM to 7.9 ± 1.4 nM ($P<0.01$) and the ventricular dialysate ACh concentration from 0.3 ± 0.1 nM in the control to 1.0 ± 0.4 nM ($P<0.01$). Atrial dialysate ACh concentrations were higher than ventricular dialysate ACh concentrations in both right and left vagal stimulation ($P<0.01$). The interaction between the stimulation and the position of probe (atrium or ventricle) was significant ($P<0.01$). There was no difference in ventricular dialysate ACh concentration between right and left vagal stimulation, but atrial dialysate ACh concentration was significantly

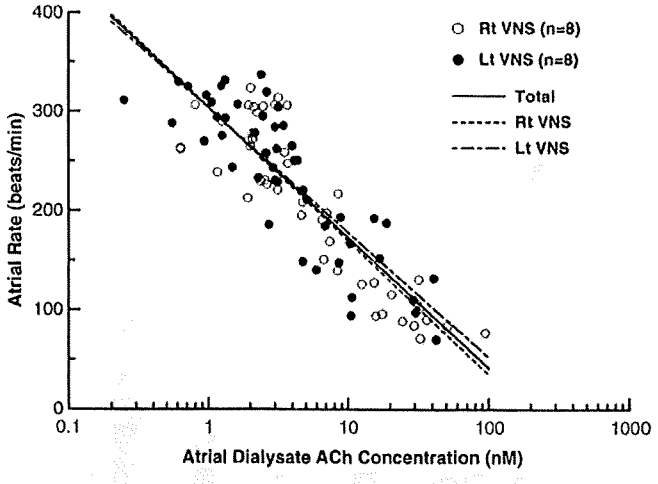

Fig. 2. Relation between dialysate ACh concentration (logarithmic scale) and atrial rate. Dialysate ACh concentration in the right atrium correlates well with atrial rate ($R^2=0.77$). Solid line, regression line fitting all 96 data points; dotted line, regression line fitting 48 data points of right vagal nerve stimulation; dot-dashed line, regression line fitting 48 data points of left vagal nerve stimulation. Rt: right; Lt: left; VNS: electrical vagal nerve stimulation.

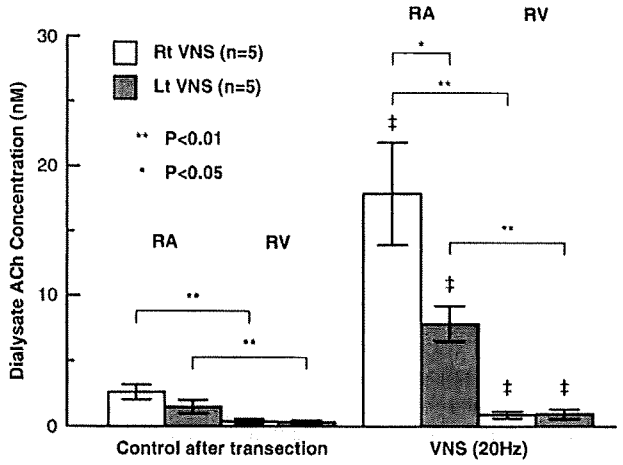

Fig. 3. Dialysate ACh concentrations in right atrium and right ventricle of controls and during electrical vagal nerve stimulation. Right vagal nerve stimulation significantly increased dialysate ACh concentration from 2.6±0.6 to 17.9±4.0 nM in the right atrium ($P<0.01$) and from 0.4±0.2 to 0.9±0.3 nM in the right ventricle ($P<0.01$). Left vagal nerve stimulation also increased dialysate ACh concentrations from 1.5±0.4 to 7.9±1.4 nM in the right atrium ($P<0.01$) and from 0.3±0.1 to 1.0±0.4 nM in the right ventricle ($P<0.01$). Dialysate ACh concentrations in the right atrium were significantly higher than those in the ventricle ($P<0.01$). Right vagal nerve stimulation increased atrial dialysate ACh concentration more than left vagal nerve stimulation ($P<0.05$). Values are means±SE; Rt: right; Lt: left; RA: right atrium; RV: right ventricle; VNS: electrical vagal nerve stimulation; *n*: number of rabbits; ‡$P<0.01$ vs. control; **$P<0.01$, *$P<0.05$.

higher during right vagal stimulation compared to left vagal stimulation ($P<0.05$).

3.3. Protocol 3

Responses of heart rate and mean arterial pressure are shown in Table 3. Both right and left vagal nerve stimulation decreased heart rate markedly before administration of hexamethonium. Administration of hexamethonium decreased heart rate significantly but mildly compared to control. Mean arterial pressure was maintained at pre-stimulation levels by continuous intravenous infusion of phenylephrine. After administration of hexamethonium, both right and left vagal nerve stimulation did not change the heart rate. Right vagal stimulation increased dialysate ACh concentration from 2.5±0.4 to 16.3±2.8 nM ($P<0.01$), but right vagal stimulation after administration of hexamethonium failed to increase ACh concentration (2.2±0.4 nM) compared to control. Likewise, left vagal stimulation increased dialysate ACh concentration from 1.5±0.3 to 8.7±1.4 nM ($P<0.01$), but left vagal stimulation after administration of hexamethonium did not increase ACh concentration (1.5±0.3 nM) compared to control (Fig. 4).

4. Discussion

We demonstrated that the microdialysis technique permitted in vivo monitoring of ACh release into the sinoatrial node from postganglionic cardiac vagal nerves. Dialysate ACh concentration in the right atrium correlated well with atrial rate and this correlation was independent of the side of vagal stimulation. These results indicate that in vivo monitoring of the myocardial interstitial ACh levels in the right atrium by microdialysis provides a useful strategy to obtain insights into the physiological roles of the vagal system in regulating heart rate.

4.1. Characteristics of atrial dialysate ACh concentration

With both right and left vagal nerve stimulation, the dialysate ACh concentration in the right atrium increased with increasing stimulus frequency and decreased to prestimulation levels after stimulation (Fig. 1). These results indicate that atrial dialysate ACh reflects ACh release from cardiac vagal nerves innervating the right atrium. Right vagal nerve stimulation decreased the atrial rate more than left stimulation at all stimulus frequencies, and right vagal nerve stimulation increased dialysate ACh concentration more than left stimulation at 10- and 20-Hz. The right atrium, including the SA node, is innervated not only by the right but also by the left vagal nerve. Ardell and Randall (1986) reported that supramaximal right and left

Table 2
Responses of heart rate and mean arterial pressure to electrical vagal nerve stimulation (protocol 2).

	Heart rate (bpm)	Mean arterial pressure (mm Hg)
Rt vagal stimulation ($n=5$)	Atrial rate (pacing rate)	
Control after transaction	305±3	74±8
VNS (20 Hz)	122±4** (304±4)	65±9*
Control after VNS	300±3	68±8
Lt vagal stimulation ($n=5$)	Atrial rate (pacing rate)	
Control after transaction	306±5	95±3
VNS (20 Hz)	168±19** (308±5)	83±1**
Control after VNS	316±8	82±2**

Values are means±SE; *n*, numbers of rabbits; Rt: right; Lt: left; VNS: electrical vagal nerve stimulation; **$P<0.01$ vs. control; *$P<0.05$ vs. control.

Table 3
Responses of heart rate and mean arterial pressure to electrical vagal nerve stimulation (protocol 3).

	Heart rate (bpm)	Mean arterial pressure (mm Hg)
Rt vagal stimulation ($n=9$)	Atrial rate (pacing rate)	
Control after transaction	292±9	70±8
VNS (20 Hz)	116±7** (299±5)	69±7
Hexamethonium iv	257±4**	84±7*
VNS after hexamethonium iv	257±4**	83±8*
Lt vagal stimulation ($n=8$)	Atrial rate (pacing rate)	
Control after transaction	317±3	79±3
VNS (20 Hz)	173±13** (313±4)	81±3
Hexamethonium iv	273±4**	87±5
VNS after hexamethonium iv	273±4**	87±4

Values are means±SE; *n*, numbers of rabbits; Rt: right; Lt: left; VNS: electrical vagal nerve stimulation; iv: intravenous administration; **$P<0.01$ vs. control; *$P<0.05$ vs. control.